IOP Conference Series: Materials Science and Engineering



# Sequential deposition method of $TiO_2/CH_3NH_3PbI_3$ films for solar cell application

IOP Conf. Series: Materials Science and Engineering **659** (2019) 012083 doi:10.1088/1757-899X/659/1/012083

# Sequential deposition method of $TiO_2/CH_3NH_3PbI_3$ films for solar cell application

**A E R T P Oliveira[1], F Bonatto[1], A K Alves[1] and C Fragassa[2]**

[1] Post-Graduation Program in Mining, Metallurgy and Materials Engineering (PPGE3M), Federal University of Rio Grande do Sul, Osvaldo Aranha 99, 90035-190, Porto Alegre, Brazil

[2] InterDepartmental Centre for Industrial Research on Advanced Applications in Mechanical Engineering & Materials Technology, Alma Mater Studiorum University of Bologna, viale Risorgimento 2, 40136 Bologna, Italy

E-mail: anne.targino@ufrgs.br

**Abstract.** Seeking to study innovative solar cell compositions with the goal to reach the highest energy efficiency level attainable, the aim of this study was to develop a route to obtain a solar cell composed by hybrid perovskite ($CH_3NH_3PbI_3$) using a sequential deposition method through the techniques of spin-coating and immersion. Initially, the deposition of $PbI_2$ thin film of was performed on a FTO/glass substrate coated with $TiO_2$, which was subsequently converted into perovskite crystals through spin coating using a $CH_3NH_3I$ solution. The influence of the $PbI_2$ layer thickness on the formation of $CH_3NH_3PbI_3$ crystals was evaluated. The hydrophilic characteristic of $TiO_2$ affects the distribution of the crystals nucleation sites, since $PbI_2$ possesses a non-polar liquid characteristic. The characterization of the perovskite thin films showed that thickness affects directly the bandgap and the surface morphology, revealing the presence of dendritic structures and acicular crystals. Both growth and coverage increased for thinner layers of $PbI_2$. It was also possible to observe an increased uniformity in the film for smaller $PbI_2$ layers.

## 1. Introduction

The development of sustainable energy sources has become critical, since most of the global energy still relies on fossil matter, whereas a scenario of an industrial sector considerably dependent on coal and the urban mobility that almost entirely leans on polluting fuels such as gasoline and diesel can be verified. Within this context, solar energy is increasingly becoming an attractive alternative, causing a major increase in research and development of more efficient and inexpensive photovoltaic devices either for industrial plants or, more recently, solar-powered zero-emission vehicles [1-3]. Aiming to explore novel and more energy-efficient manufacturing alternatives for solar cells, recent literature have focused on perfecting techniques of deposition of different thin films over the solar cell substrate to allow a higher absoption of light and, consequently, enhanced levels of output energy.

The use of organic-inorganic perovskite halides as an absorbable layer in thin film solar cells started in 2009, resulting in a PV device with 3.1% efficiency [4]. In recent years, the rapid evolution of the device has led to a modification of its structure, with a large increase in efficiency, reaching values above 23.7% [5]. This organometallic material has been widely explored due to the singular

characteristics of the perovskite material such as excellent and adjustable optical properties by controlling chemical compositions [6], ambipolar load transport [7], and very long diffusion lengths [8].

Deposition of perovskite halide thin films can be performed by vapor phase deposition, solution-gel chemistry approaches, one step deposition, and two-step solution synthesis [9-11]. Usually, perovskite is synthesized by combining two precursors, an organic and other inorganic, which can be combined by different deposition routes [12]. Most deposition methods are based on the same principle: the combination of an organic component iodide methylammonium (MAI), with an inorganic component, such as iodide or lead chloride ($PbI_2$ or $PbCl_2$), to produce a perovskite ($CH_3NH_3PbI_3$ or $CH_3NH_3PbI_{3-x}Cl_x$, respectively) [13].

In this work, we have compared the velocity of deposition of halide perovskite ($CH_3NH_3Pb_2I_3$) using a simple two-step method of deposition, over a mesoporous $TiO_2$ layer deposited in F doped $SnO_2$, to access morphological and optical properties for future use in solar cells.

## 2. Materials and methods

### *2.1. Preparation of precursor solutions*

For the preparation of the $CH_3NH_3PbI_3$ films it was used glass covered with FTO (Fluorine doped Tin Oxide) with measurements of 2.5 cm long and 1 cm wide. The slides were immersed in acetone and placed on the ultrasound over 5 minutes for cleaning. They were washed with distilled water and then subjected to a temperature of 400 °C for 30 min to eliminate any organic matter that was present. A $TiO_2$ paste was prepared for the deposition of $TiO_2$ by spin coating. The paste was obtained by grinding 50 g of $TiO_2$-P25 (Evonik), 20 g of titanium isopropoxide (97 %, Sigma-Aldrich), 2.5 g of carboxi methyl cellulose (Sigma-Aldrich), 80 mL of terpineol (Sigma-Aldrich), 4 mL of acetyl acetonate (Sigma-Aldrich) and 5 mL of ethanol (99 %, Zeppelin) for a period of 12 h, so the paste was fully homogenized. For the preparation of $PbI_2$ solution, it was used a two-steps methodology: 1 M solution was obtained dissolving $PbI_2$ in anhydrous N, N-Dimethylmethanamide under agitation at a temperature of 70 °C. The precursor solution was ready for use when the salt was completely dissolved and with a translucent yellow color. For the second stage of two-step deposition, a solution was prepared composed of 10 mg/mL $CH_3NH_3I$ in anhydrous isopropanol, agitated for a period of 10 min, in which all iodine methylammonium was dissolved.

### *2.2. Deposition in thin film*

The $TiO_2$ mesoporous layer was made from a dissolution of the $TiO_2$ paste in ethanol with a proportion of 2:7. The solution was deposited at 3000 rpm per 20 s. The obtained film was dried at 125 °C for 10 min and then sintered 450 °C for 30 min. The perovskite layer was prepared using sequential two steps method describe by Burschka et al [11], but the second step was modified using the spin coating technique. The $PbI_2$ solution deposition was performed by spin coating, with different speeds for obtaining different thicknesses: 2000, 3000 and 4000 rpm, with two consecutive depositions. After this step, a 10-minute drying was made on a heating plate at 70 °C. Subsequently, each sample was covered with a solution of MAI in a spin coating process using a speed of 2000 rpm, followed by drying the film at 100 °C for 30 min. The film samples were named as PV-2, PV-3, PV-4 according to their respective deposition speeds: 2000, 3000 or 4000 rpm. The whole experiment was carried out at ambient condition (room temperature and open atmosphere).

## 3. Results and Discussion

For morphological characterization, scanning electron microscopy (SEM) was used to analyze the layer thickness influence of the $PbI_2$ films. The comparisons of the results obtained under the effect of the variation of deposition parameters are presented in Figure 1. The analyses revealed that the samples are homogeneous (without cracks) and with uniform appearance throughout the whole surface. It can be seen in Figure 1 (a), (c) and (e) that as the $PbI_2$ deposition velocity was increased,

there was a growth of crystals. The hydrophilic character of $TiO_2$ [14,15] possibly affects the distribution of the nucleation sites of the crystals originating from the $PbI_2$. Figure 1 (e) revealed the presence of dendritic structures and needle-shaped crystals. There is the formation of perovskite grains for the speeds of 2000 and 3000 rpm (Figure 1 a to d). When 4000 rpm was used (Figure 1 f) there is no presence of these grains, and only dendritic structures are formed. This behavior of dendritic formation can be explained by the rapid cooling of the $PbI_2$ solution due to its higher velocity of deposition. It is also possible to observe the mesoporous layer of $TiO_2$ below the grains and dendrites of formed perovskites.

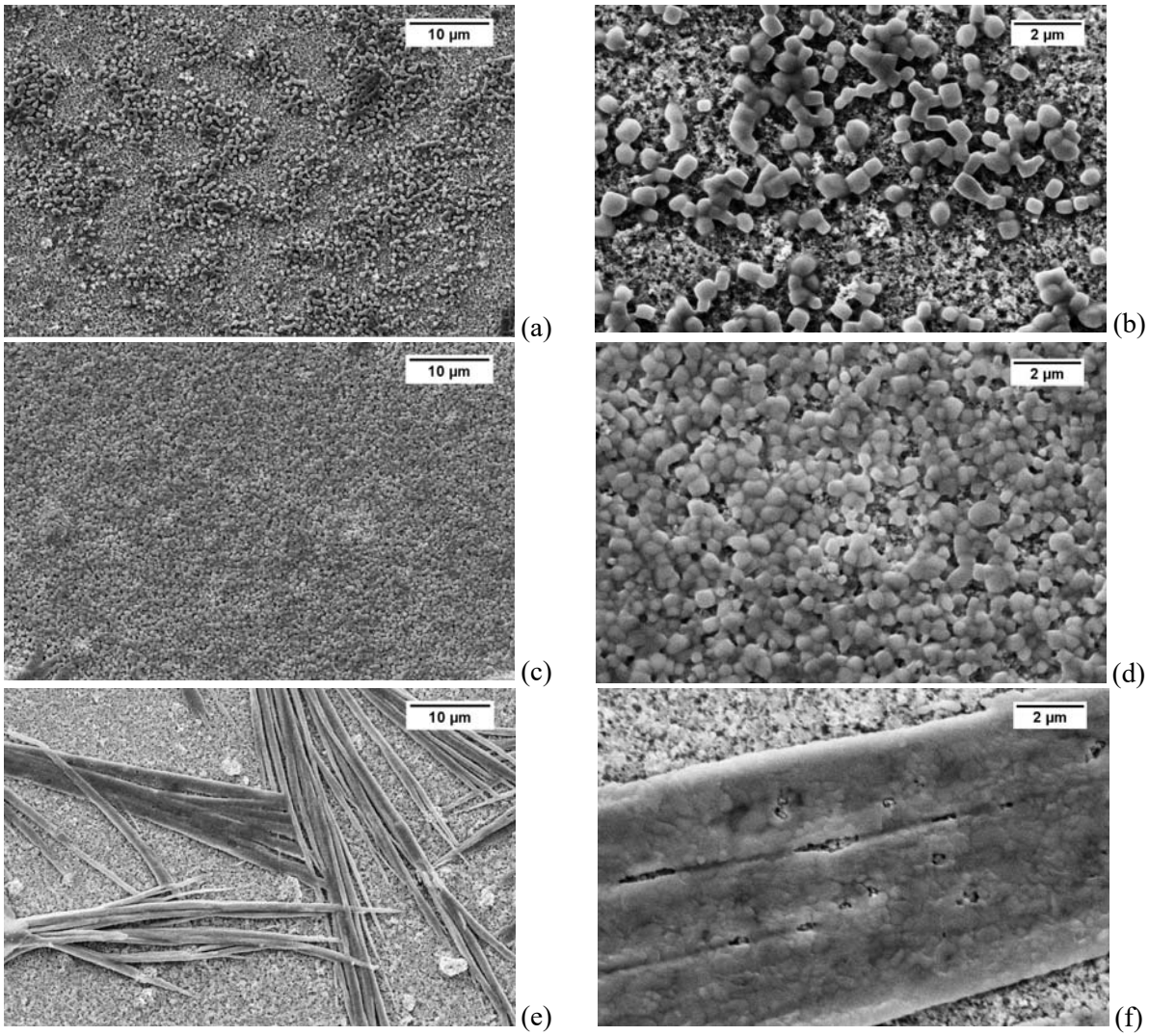


**Figure 1.** SEM images of $CH_3NH_3PbI_3/TiO_2$ films. Deposition velocity: (a)-(b) 2000 rpm, (c)-(d) 3000 rpm and (e)-(f) 4000 rpm.

The optical bands for $CH_3NH_3PbI_3/TiO_2/FTO$ films were determined by diffuse reflectance measurements (Figures 2 a, b and c). The measure of the extinction coefficient $\alpha$ , which is proportional to F(R), is calculated using the reflectance data according to the equation Kubelka-Munk [16,17], $F(R) \sim \alpha = (1-R)^2/2R$, where R is the percentage of reflected light, A is the energy of the incident photon (hν).The energy of the optical band gap (Eg) are related to the transformed Kubelka-Munk function, alpha $(h\nu) = B\ (h\nu - Eg)^n$, where B is the absorption constant, Eg is the band gap

energy and n is the power index that is related to the optical absorption, which in this case is related to a indirect transition and have the value of 1/2. According to other studies, the band gap of the $TiO_2$ determined based on the indirect transition is between 3.17 and 3.28 eV [18], due to the higher presence of the anatase phase. The $CH_3NH_3PbI_3$ bandgap is equivalent to 1.5 eV [6], which is formed between the orbital Pb and I. The calculated values for the optical band gaps are 3.15; 3.3 and 2.7 eV respectively, for PV-4, PV-3, PV-2 samples. It was observed that for higher deposition speeds, the bandgap is directly related to the presence of $TiO_2$, because the perovskite layer is thinner. For the deposition in lower velocity, the band gap was estimated between the values 1.5 and 3.2 eV due to the greater presence of perovskite.

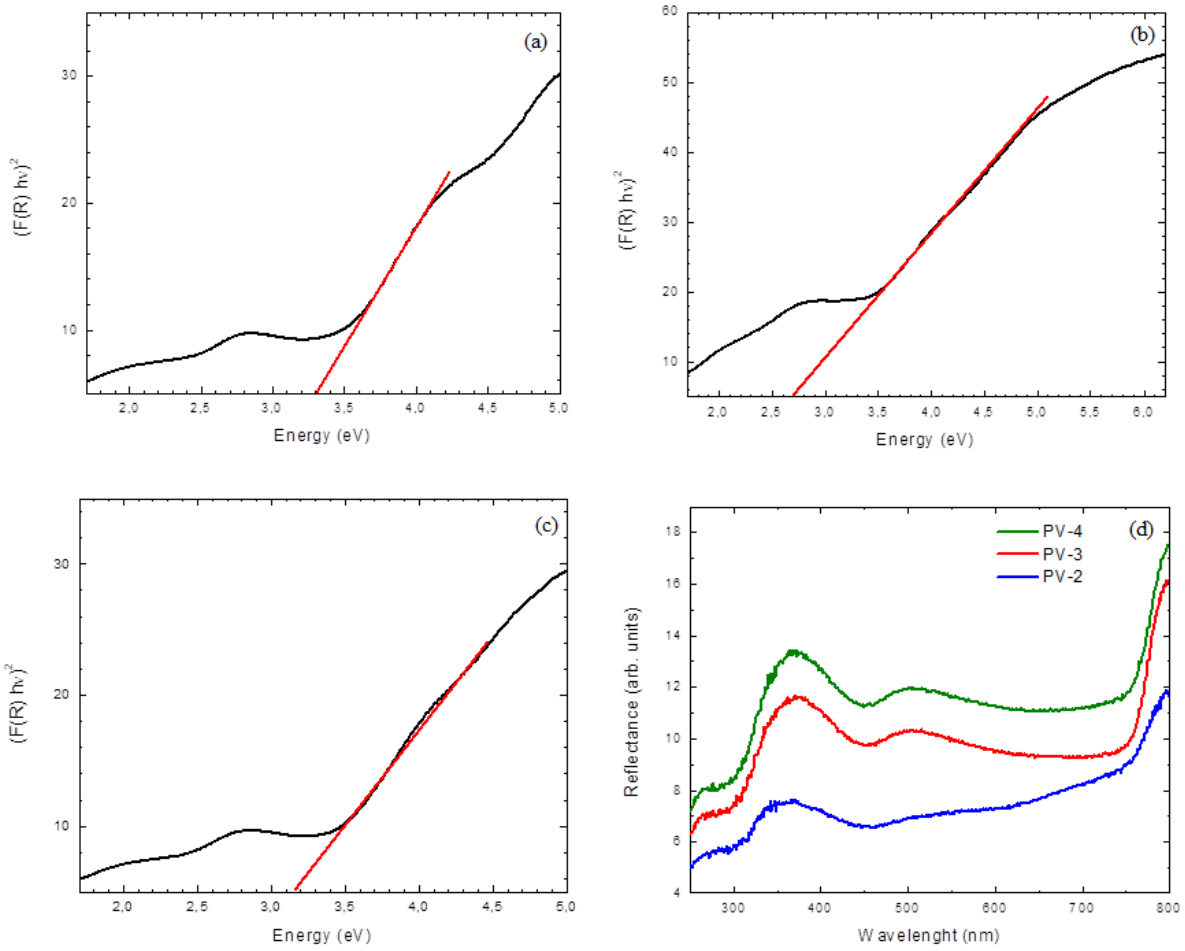


**Figure 2.** Transformed Kubelka-Munk spectrum of the $CH_3NH_3PbI_3$-sensitized $TiO_2$ film, $PbI_2$ depositions conditions: (a) 2000 rpm, (b) 3000 rpm, (c) 4000 rpm; (d) diffuse reflectance spectrum of the $CH_3NH_3PbI_3$-sensitized $TiO_2$ film.

The UV-vis absorption spectra of $CH_3NH_3PbI_3$ films deposited on $TiO_2$ were depicted in Figure 3a. As can be seen in the diagram, the absorption spectra in the UV region have prominent peaks at 280 nm for the PV-2 , for PV-3 around 282 nm and for PV-4 around 281 nm indicating a perovskite formation [19]. The film prepared at 3000 rpm presents a greater absorption compared to the other films corroborating the results of SEM where it is possible to observe a greater formation of perovskite. In the other films, there is no significant difference in the absorption spectrum.

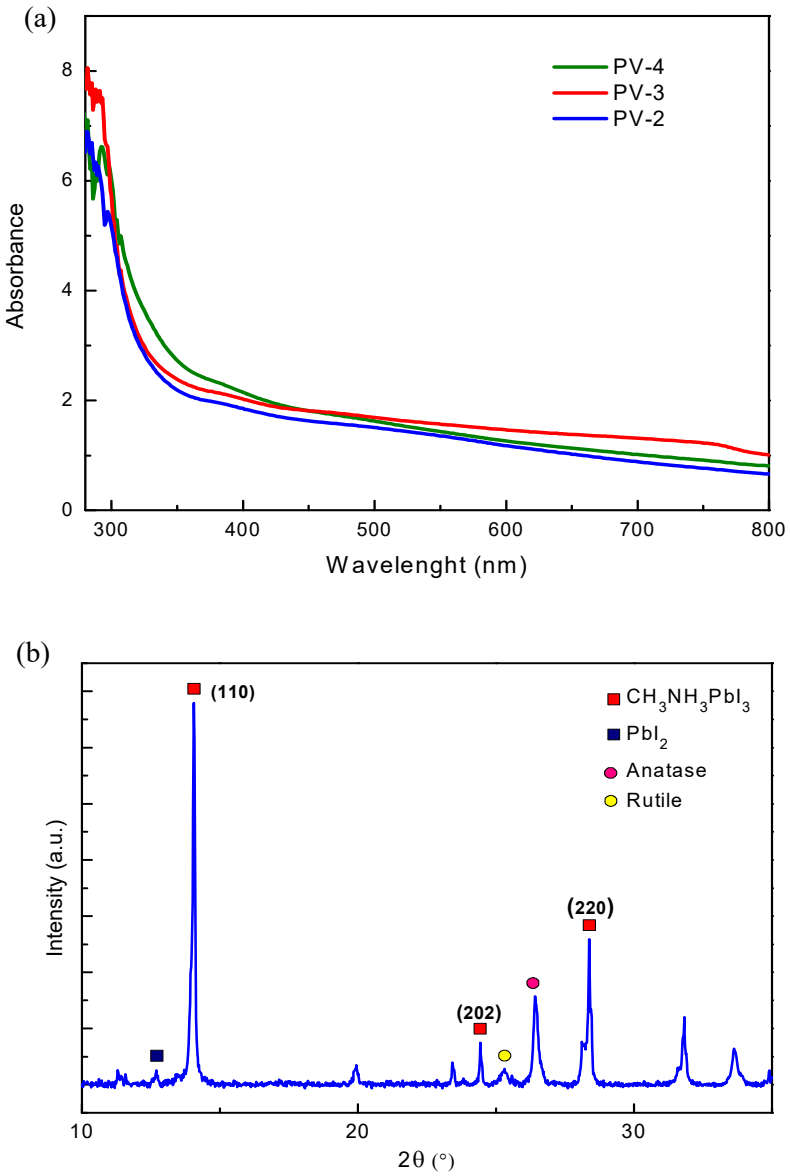


**Figure 3.** (a) UV-Vis absorption spectra of $CH_3NH_3PbI_3/TiO_2$ films. (b) XRD pattern of $TiO_2$/ $CH_3NH_3PbI_3$ thin film on FTO-glass.

The X-ray diffractogram for PV-3 is shown in Figure 3b. The diffractograms of the other samples were very similar to the PV-3 spectra. It can be noted that the diffraction signal related to the formation of perovskite $CH_3NH_3PbI_3$ in $2\theta = 14°$ is the most intense, and confirms the high crystallinity of the synthesized film. In addition, a weak signal at $2\theta = 12.4$ °, related to the precursor $PbI_2$, can be seen, indicating that the majority of $PbI_2$ precursor has been transformed into perovskite. Usually, the presence of $PbI_2$ is related to the degradation of the perovskite in the presence of moisture [20]. The XRD results indicates that the perovskite film has a good stability because only a residual presence of the precursor was identified. Finally, the perovskite planes (202) and (220), in $2\theta = 24.4°$ and $2\theta = 28.3°$, respectively, can be identified, in addition to the anatase peaks at $2\theta = 25.2°$ and rutile at $2\theta = 26.4°$, belonging to $TiO_2$ film from the substrate [21]. To calculate the average grain size of the

perovskite, the Scherrer equation was used, considering the value of fwhm for the peak associated with the plane (110). Analysis of this data provided an average grain size of approximately 91 ± 3 nm.

## 4. Conclusion

In this study, the influence of the thickness of $PbI_2$ layers on FTO/$TiO_2$/$CH_3NH_3PbI_3$ films was investigated. The surface morphology of the films showed that with the increase of deposition velocity, there is a variation in the formation of perovkskite crystals, which can be explained by the rapid cooling of the $PbI_2$ solution in the FTO substrate. The PV-3 sample was the one with the better homogenous distribution of perovskite. There was a variation in the optical band gap for the lower velocity layer due to the greater presence of deposited material ($PbI_2$). The sample PV-3 had a more expressive absorption due to the greater amount of perovskite formed. Little crystallographic variation was observed, confirming the perovskite formation for all samples. The thin films have been synthesized successfully indicating that it is possible to employ this film in a future use for solar cells. The methodology allows fast production of thin films with lower cost due to their possible production in ambient conditions.

## Acknowledgment

The authors would like to thank the Coordination for the Improvement of Higher Education Personnel – CAPES, the National Council for Scientific and Technological Development – CNPq and the Foundation of Support to Research of the State of Rio Grande do Sul – FAPERGS for the financial support. The present paper was presented inside the '*Toward a Sustainable Mobility*' special session as part of the '*Two Seats for a Solar Car*' research project, an action funded by the Italian Ministry of Foreign Affairs and International Cooperation within the Executive Programme of Cooperation in the field of Science and Technology between the Italian Republic and the Republic of Serbia.

## References

[1] Minak G, Brugo T M, Fragassa C, Pavlovic A, de Camargo F V and Zavatta N 2019 Structural Design and Manufacturing of a Cruiser Class Solar Vehicle, *Journal of Visual Experiments* **143** e58525, doi:10.3791/58525

[2] Minak G, Fragassa C and de Camargo F V 2017 *A brief review on determinant aspects in energy efficient solar car design and manufacturing*, International Conference on Sustainable Design and Manufacturing, Bologna, Italy, April 26 – 28, pp. 847-856

[3] de Camargo F V, Giacometti M and Pavlovic A 2017 *Increasing the energy efficiency in solar vehicles by using composite materials in the front suspension*, International Conference on Sustainable Design and Manufacturing, Bologna, Italy, April 26 – 28, pp. 801-811

[4] Noh M F M, The C H, Daik, Lim E L, Yap C C, Ibrahim M A, Ludin N A, Yusoff A R M, Jang J and Teridi M A M 2018 The architecture of the electron transport layer for a perovskite solar cell, *J. Mater. Chem.* C **6** 682

[5] Jena A K, Kulkarni A and Miyasaka T 2019 Halide perovskite photovoltaics: background, status, and future prospects, *Chem. Rev.* **119** 3036-3103

[6] Noh J H, Im S H, Heo J H, Mandal T N and Seok S I 2013 Chemical Management for Colorful, Efficient, and Stable Inorganic-Organic Hybrid Nanostructured Solar Cells, *Nano Letters* **13**(4) 1764-1769

[7] Heo J H, Im S H, Noh J H, Mandal T N, Lim C S, Chang J A, Lee Y H, Kim H J, Sarkar A, Nazeeruddin M K, Grätzel M and Seok S I 2013 Efficient inorganic–organic hybrid heterojunction solar cells containing perovskite compound and polymeric hole conductor, *Nat Photonics* **7** 487–492

[8] Xing G, Mathews N, Sun S, Lim S S, Lam Y M, Gratzel M, Mhaisalkar S and Sum T C 2013 Long-range balanced electron- and hole-transport lengths in organic-inorganic $CH_3NH_3PbI_3$, *Science* **342** 344

[9] Lee M M, Teuscher J, Miyasaka T, Murakami T N and Snaith H J 2012 Efficient hybrid solar cells based on meso-superstructured organometal halide perovskites, S*cience* **338**(6107) 643-647

[10] Chen Q, Zhou H, Hong Z, Luo S, Duan H S, Wang H H, Liu Y, Li G and Yang Y 2014 Planar heterojunction perovskite solar cells via vapor-assisted solution process, *J. Am. Chem. Soc.* **136**(2) 622-625

[11] Burschka J, Pellet N, Moon S J, Humphry-Baker R, Gao P, Nazeeruddin M K and M. Grätzel 2013 Sequential deposition as a route to high-performance perovskite-sensitized solar cells, *Nature* **499** (7458) 316–319

[12] Matthews P D, Lewis D J and O'Brien P 2017 Updating the Road Map to Metal-Halide Perovskites for Photovoltaics, *J. Mater. Chem.* A **5**(33) 17135–17150

[13] Stranks S D, Nayak P K, Zhang W, Stergiopoulos T and Snaith H J 2015 Formation of Thin Films of Organic–Inorganic Perovskites for High-Efficiency Solar Cells, *Angewandte. Chem. Int*. **5** 3240

[14] Sakai N, Fujishima A, Watanabe T and Hashimoto K 2003 Quantitative Evaluation of the Photoinduced Hydrophilic Conversion Properties of $TiO_2$ Thin Film Surfaces by the Reciprocal of Contact Angle, *The Journal of Physical Chemistry* B **107**(4) 1028–1035

[15] Jesus M A M L, Timòb G, Agustín-Sáenz C, Braceras I, Cornelli M and Ferreira A M 2018 Anti-soiling coatings for solar cell cover glass: Climate and surface properties influence, *Solar Energy Materials and Solar Cells* **185**(2018) 517–523

[16] Kortum G F A 1969 *Reflectance Spectroscopy: Principles, Methods, Applications*, Springer

[17] Simmons L E 1975 Diffuse reflectance spectroscopy: a comparison of the theories, *Appllied Optics* **14**(6) 1380–1386

[18] Lin H, Huang C P, Li W, Ni C, Ismat S S and Tseng Y-H 2006 Size dependency of nanocrystalline TiO2 on its optical property and photocatalytic reactivity exemplified by 2-chlorophenol, *Applied Catalysis B: Environmental* 68 1-11

[19] Eze V O and Mori T 2016 Organic-Inorganic Hybrid Perovskite Solar Cells Using Hole Transport Layer Based on α-Naphthyl Diamine Derivative, *Journal of Photopolymer Science and Technology* **29**(4) 581–586

[20] Mokhtar M Z , Chen M, Whittaker E, Hamilton B, Aristidou N, Ramadan S, Gholinia A, Haque S A, O'Brien P and Saunders B R 2017 $CH_3NH_3PbI_3$ films prepared by combining 1- and 2-step deposition: how crystal growth conditions affect properties, *Phys. Chem. Chem. Phys.* **19** 7204 -7214

[21] Jeong B, Hwang I, Cho S H, Kim E H, Cha S, Lee J, Kang H S, Cho S M, Choi H, Parl 2016 Solvent-assisted gel printing for micropatterning thin organic–inorganic hybrid perovskite films, *ACS Nano* **10**(9) 9026-9035